Journal of Sound and Vibration (2000) **230**(5), 1147–1163
doi:10.1006/1999.2662, available online at http://www.idealibrary.com IDEAL®

COUPLED FREQUENCIES OF A FRICTIONLESS LIQUID IN A CIRCULAR CYLINDRICAL TANK WITH AN ELASTIC PARTIAL SURFACE COVER

H. F. BAUER

Institute für Raumfahrttechnik, Universität der Bundeswehr München, D-85577 Neubiberg, Germany

AND

K. KOMATSU

Structural Mechanics Division, National Aerospace Laboratory, 7-44-1, *Jindaiji-Higashi, Chofu, Tokyo* 182-8522, *Japan*

(*Received* 22 *March* 1999, *and in final form* 20 *September* 1999)

If the free liquid surface in a circular cylindrical container is partially covered by a structural element, the natural frequencies of the liquid are exhibiting increased magnitude. In addition, a much calmer liquid motion results from such coverages. In order to save structural weight, such devices may exhibit elastic behavior. The following investigation treats the hydroelastic problem of the interaction of liquid sloshing with an elastic annular plate structure attached to the cylindrical sidewall. It was found that decreasing rigidity of the annular plate exhibits less increase of the natural frequencies than that of a rigid plate. The increase of the plate width and a decrease of the Bond number increases the natural frequency drastically.

1. INTRODUCTION

With the increasing size of space vehicles and airplanes, the focus being on lighter structure and increased payloads, and with their larger amount of propellants and larger propellant container dimensions, the effect of propellant sloshing upon the performance, control and stability of such vehicles is becoming more pronounced and in many cases dangerous for the flight mission. These sloshing effects have led to great difficulties during the ascending phase of missiles and space vehicles and have created painful failures in the early years of spaceflight. The problem that appeared in all space vehicles is the closeness of the control frequency to the fundamental sloshing frequency, rendering with a tilt program and the wind gust inputs, a continuous excitation of the propellant oscillations. This is particularly dangerous since the fundamental sloshing mass participating in the oscillations is

0022-460X/00/101147 + 17 $35.00/0

very large and may by its constant motion during the ascending phase require swivel engine deflections which may no longer be available in that magnitude. This may therefore lead to the non-controllability and destruction of the total vehicle [1]. For the reduction of liquid amplitudes, liquid forces and moments on the vehicle some baffle devices have been useful to guarantee a successful flight performance. The most frequently used baffles were ring baffles of certain width which provided enough damping from the propellant motion for a safe flight [2]. They also calm down the motion in the container.

The problem of liquid oscillations in various container geometries has been treated extensively and may be found in references [3–10]. It was also found that the location of the container had a decisive influence upon the stability of the overall vehicle. A location between the mass center and the center of instantaneous rotation required more damping and therefore larger baffle width. This cannot be accomplished for all containers in a multistage space vehicle to keep them out of this range. Another diminishing effect of the propellant upon the stability of the vehicle may be accomplished by introducing longitudinal cross-walls, i.e., subdivision of the container, such as quarter tank [11] or $\frac{1}{8}$-tank arrangement [12]. In this case the sloshing mass is reduced drastically and the sloshing frequencies are increased, showing the destabilizing effect of propellant, sloshing can be handled by this method quite effectively. The disadvantage of this method, however, is quite obvious, since it requires a large amount of additional structural weight, and therefore reduces the payload considerably.

To avoid such penalties, the following investigation uses light structural elements, which partly cover the free liquid surface of the propellant (see Figure 1). This way the fundamental natural frequency is shifted to larger magnitude and yields in addition a calmer motion of the liquid [13], a fact that also reduces the sloshing mass participating in the oscillation. This shall be of great benefit to the overall performance of the space vehicle. In addition, there appears a valuable side-effect for the proper pressurization of the gaseous space in a container with cryogenic propellant. The reduced motion of the propellant requires, due to less sloshing at the free surface of the propellant, less pressurization gas in the space above the propellant to maintain the proper pressure head for the fuel pumps.

To reduce as much as possible the weight penalties being introduced by ring baffles their structure should be as light as possible, but still providing the effect of natural frequency increase and reduction of the liquid motion. These depend on the elasticity and the width of the annular structure. For this reason the structural element covering partly the free liquid surface has been treated as an elastic annular plate in interaction with the sloshing liquid. In the following, we therefore investigate the hydroelastic problem of a non-viscous liquid in a rigid circular cylindrical container of which the free liquid surface is obstructed by an elastic annular plate of certain width. The rigidity of the annular plate as well as its width play, of course, a decisive role in the effectiveness of such a device. In addition, we also consider the influence of decreasing longitudinal acceleration g, which make the surface tension a predominant factor. This is expressed by decreasing Bond number $\mathrm{Bo} = \rho g a^2/\sigma$. We shall here investigate only an elastic annular plate attached to the container side wall. It is, however, possible to perform the following

investigation for other coverage of the free surface, such as an annular plate concentrically located and being very efficient for axial oscillations of the system.

It may be mentioned that in a multistage aerospace vehicle some containers are located exactly in the range between the center of mass and the center of instantaneous rotation, where large damping magnitudes or shifting of the natural frequencies combined with the reduction of the sloshing masses are required for stable flight conditions. Especially for such containers the coverage of the free propellant surface with a structural element will calm the liquid motion considerably. This makes the natural frequencies deviate from the control frequency towards the higher side and reduces the sloshing masses with relatively low structural weight additions.

It may also be of interest to remark that the results of the following investigation could be used for checking numerical methods [14–16], such as finite elements or others, applicable to more complex geometries. It should also be mentioned that the liquid motion in ship-tankers, railroad- and road-tankers could be considerably calmed down by such additional surface structures, thus resulting in an enhanced and failsafe handling of the vehicle. The discretization method is advantageous in many respects since it may be easily applied by replacing some equations by others.

2. BASIC EQUATIONS

A circular cylindrical container of diameter $2a$ (see Figure 1) is filled to a height h with an incompressible and frictionless liquid of density ρ. The container bottom at $z = -h$ and the side wall at $r = a$ are considered as solid walls, while the free surface at $z = 0$ is partially covered by an elastic plate. If the liquid is assumed in

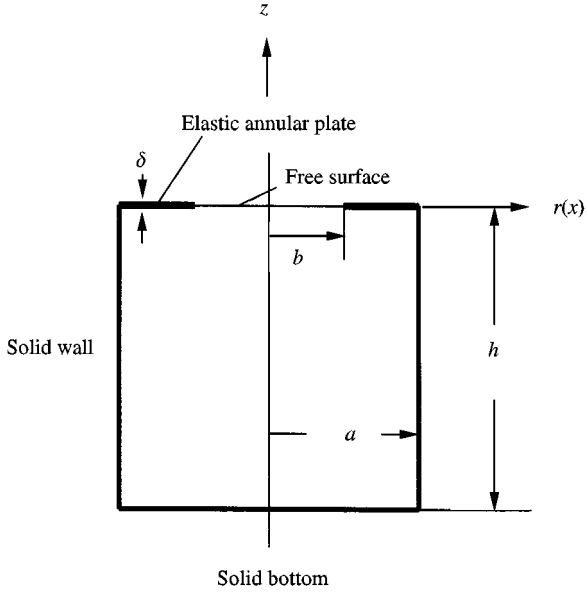

Figure 1. Geometry and co-ordinates of the hydroelastic system.

irrotational motion (**curl** $\vec{v} = 0$), the velocity distribution may be presented as a gradient of a velocity potential $\phi(r, \varphi, z, t)$, i.e., as $\vec{v} = \mathbf{grad}\ \phi$. Then the continuity equation $\mathbf{div}\,\vec{v} = 0$ yields the Laplace equation (a list of nomenclature is given in Appendix A)

$$\frac{\partial^2\phi}{\partial r^2} + \frac{1}{r}\frac{\partial\phi}{\partial r} + \frac{1}{r^2}\frac{\partial^2\phi}{\partial\varphi^2} + \frac{\partial^2\phi}{\partial z^2} = 0, \tag{1}$$

which has to be satisfied by

$$\partial\phi/\partial r = 0 \quad \text{at the tank wall } r = a \tag{2}$$

and

$$\partial\phi/\partial z = 0 \quad \text{at the tank bottom } z = -h. \tag{3}$$

If the free liquid surface at $z = 0$ is partially covered by an annular elastic plate of width $w = a(1 - k)$ in the range $k \leqslant r/a \leqslant 1$, the boundary condition at $z = 0$ is given by ($k \equiv b/a$)

$$\frac{\partial^2\phi}{\partial t^2} + g\frac{\partial\phi}{\partial z} + \frac{\sigma}{\rho}\frac{\partial^3\phi}{\partial z^3} = 0 \quad \text{at } z = 0 \quad \text{in the range} \quad 0 \leqslant r/a < k \tag{4}$$

and the compatibility condition

$$\partial\bar{\zeta}/\partial t = \partial\phi/\partial z \quad \text{at } z = 0 \text{ in the range } k \leqslant r/a \leqslant 1. \tag{5}$$

In these equations, g is the gravity constant, σ the liquid surface tension and $\bar{\zeta}(r, \varphi, t)$ the displacement of the elastic plate, which has the equation of motion

$$D\left[\frac{\partial^2}{\partial r^2} + \frac{1}{r}\frac{\partial}{\partial r} + \frac{1}{r^2}\frac{\partial^2}{\partial\varphi^2}\right]^2\bar{\zeta} + \mu\frac{\partial^2\bar{\zeta}}{\partial t^2} = p(r, \varphi, z, t)|_{z=\bar{\zeta}}, \tag{6}$$

where $D = E\delta^3/12(1 - \nu^2)$ is the flexural rigidity of the plate, ν the Poisson ratio, E is Young's modulus of elasticity, δ the thickness of the plate, and μ the mass per unit area of the plate. The pressure p stems from the liquid and is given by

$$p(r, \varphi, z, t)|_{z=\bar{\zeta}} = -\rho(\partial\phi/\partial t) - \rho\bar{g}\bar{\zeta} \quad \text{at } z = 0. \tag{7}$$

The boundary conditions of the clamped–free annular elastic plate are presented by

$$\bar{\zeta} = 0 \quad \text{and} \quad \partial\bar{\zeta}/\partial r = 0 \quad \text{at } r/a = 1 \tag{8a, b}$$

for a clamped boundary, and for a free boundary

$$\frac{\partial^2\bar{\zeta}}{\partial r^2} + \nu\left(\frac{1}{r}\frac{\partial\bar{\zeta}}{\partial r} + \frac{1}{r^2}\frac{\partial^2\bar{\zeta}}{\partial\varphi^2}\right) = 0 \quad \text{at} \quad \frac{r}{a} = k, \tag{9a}$$

$$\frac{\partial}{\partial r}\left(\frac{\partial^2\bar{\zeta}}{\partial r^2} + \frac{1}{r}\frac{\partial\bar{\zeta}}{\partial r} + \frac{1}{r^2}\frac{\partial^2\bar{\zeta}}{\partial\varphi^2}\right) + \frac{(1-\nu)}{r}\frac{\partial}{\partial r}\left(\frac{1}{r}\frac{\partial^2\bar{\zeta}}{\partial\varphi^2}\right) = 0 \quad \text{at} \quad \frac{r}{a} = k. \tag{9b}$$

Equations (1)–(9) represent the hydroelastic problem.

3. METHOD OF SOLUTION

We shall treat here the free coupled oscillations and the response of the coupled system to translational excitation in the x direction.

3.1. COUPLED FREE OSCILLATIONS

For free coupled oscillations one has to solve Laplace's equation (1) together with the wall and bottom conditions (2) and (3) yielding the velocity potential

$$\phi(r, \varphi, z, t) = \sum_{m=0}^{\infty}\sum_{n=1}^{\infty}\phi_{mn}\cosh\left[\frac{\varepsilon_{mn}}{a}(z+h)\right]\mathrm{J}_m\left(\varepsilon_{mn}\frac{r}{a}\right)\cos m\varphi\ \mathrm{e}^{\mathrm{i}\omega t}, \tag{10}$$

where ε_{mn} are the roots of the first derivative of the Bessel function of order m and the first kind, i.e., $\mathrm{J}'_m(\varepsilon) = 0$. This renders the pressure distribution (at $z = 0$)

$$p = -\mathrm{i}\rho\omega\sum_{m=0}^{\infty}\sum_{n=1}^{\infty}\phi_{mn}\cosh\left(\varepsilon_{mn}\frac{h}{a}\right)\mathrm{J}_m\left(\varepsilon_{mn}\frac{r}{a}\right)\cos m\varphi\ \mathrm{e}^{\mathrm{i}\omega t} - \rho g\bar{\zeta}. \tag{11}$$

With the normal displacement of the annular elastic plate

$$\bar{\zeta}(r, \varphi, t) = \sum_{m=0}^{\infty}\bar{\zeta}_m(r)\cos m\varphi\ \mathrm{e}^{\mathrm{i}\omega t}, \tag{12}$$

the equation of motion of the plate yields the ordinary inhomogeneous differential equation

$$\left[\frac{\mathrm{d}^2}{\mathrm{d}r^2} + \frac{1}{r}\frac{\mathrm{d}}{\mathrm{d}r} - \frac{m^2}{r^2}\right]^2\bar{\zeta}_m - \left(\frac{\mu\omega^2 - \rho g}{D}\right)\bar{\zeta}_m = -\frac{\mathrm{i}\rho\omega}{D}\sum_{n=1}^{\infty}\phi_{mn}\cosh\left(\varepsilon_{mn}\frac{h}{a}\right)\mathrm{J}_m\left(\varepsilon_{mn}\frac{r}{a}\right), \tag{13}$$

which has to be solved with the boundary conditions of the plate

$$\bar{\zeta}_m = 0 \quad \text{and} \quad \mathrm{d}\bar{\zeta}_m/\mathrm{d}r = 0 \quad \text{at} \quad r/a = 1 \tag{14a, b}$$

and

$$\frac{\mathrm{d}^2\bar{\zeta}_m}{\mathrm{d}r^2} + v\left[\frac{1}{r}\frac{\mathrm{d}\bar{\zeta}_m}{\mathrm{d}r} - \frac{m^2}{r^2}\bar{\zeta}_m\right] = 0 \quad \text{at} \quad \frac{r}{a} = k, \tag{15a}$$

$$\frac{\mathrm{d}}{\mathrm{d}r}\left(\frac{\mathrm{d}^2\bar{\zeta}_m}{\mathrm{d}r^2} + \frac{1}{r}\frac{\mathrm{d}\bar{\zeta}_m}{\mathrm{d}r} - \frac{m^2}{r^2}\bar{\zeta}_m\right) - \frac{(1-v)}{r}\frac{\mathrm{d}}{\mathrm{d}r}\left(\frac{m^2}{r}\bar{\zeta}_m\right) = 0 \quad \text{at} \quad \frac{r}{a} = k. \tag{15b}$$

The solution of equation (13) is, with $\beta^4 = a^4(\rho g - \mu\omega^2)/D$, given by

$$\bar{\zeta}_m(r) = A_m \mathrm{J}_m\left(\beta\frac{r}{a}\sqrt{\mathrm{i}}\right) + B_m \mathrm{Y}_m\left(\beta\frac{r}{a}\sqrt{\mathrm{i}}\right) + C_m \mathrm{J}_m\left(\beta\frac{r}{a}\sqrt{-\mathrm{i}}\right)$$
$$+ D_m Y_m\left(\beta\frac{r}{a}\sqrt{-\mathrm{i}}\right) - \frac{\mathrm{i}\rho\omega a^4}{D}\sum_{n=1}^{\infty}\phi_{mn}\frac{\cosh(\varepsilon_{mn}h/a)\mathrm{J}_m(\varepsilon_{mn}r/a)}{\beta^4 + \varepsilon_{mn}^4} \tag{16}$$

Introducing the above four boundary conditions (14) and (15) yields

$$A_m \mathrm{J}_m(\beta\sqrt{\mathrm{i}}) + B_m \mathrm{Y}_m(\beta\sqrt{\mathrm{i}}) + C_m \mathrm{J}_m(\beta\sqrt{-\mathrm{i}}) + D_m \mathrm{Y}_m(\beta\sqrt{-\mathrm{i}})$$
$$- \frac{\omega^*}{\mu^*}\sum_{n=1}^{\infty}\phi_{mn}^*\frac{\cosh(\varepsilon_{mn}(h/a)\mathrm{J}_m(\varepsilon_{mn})}{\beta^4 + \varepsilon_{mn}^4} = 0, \tag{17}$$

$$\sqrt{\mathrm{i}}\{A_m \mathrm{J}'_m(\beta\sqrt{\mathrm{i}}) + B_m \mathrm{Y}'_m(\beta\sqrt{\mathrm{i}})\} + \sqrt{-\mathrm{i}}\{C_m \mathrm{J}'_m(\beta\sqrt{-\mathrm{i}}) + D_m \mathrm{Y}'_m(\beta\sqrt{-\mathrm{i}})\} = 0, \tag{18}$$

$$A_m\left[\frac{(v-1)}{k\beta}\sqrt{\mathrm{i}}\mathrm{J}'_m(k\beta\sqrt{\mathrm{i}}) - \mathrm{i}\mathrm{J}_m(k\beta\sqrt{\mathrm{i}}) - \frac{(v-1)m^2}{k^2\beta^2}\mathrm{J}_m(k\beta\sqrt{\mathrm{i}})\right]$$
$$+ B_m\left[\frac{(v-1)}{k\beta}\sqrt{\mathrm{i}}\mathrm{Y}'_m(k\beta\sqrt{\mathrm{i}}) - \mathrm{i}\mathrm{Y}_m(k\beta\sqrt{\mathrm{i}}) - \frac{(v-1)m^2}{k^2\beta^2}\mathrm{Y}_m(k\beta\sqrt{\mathrm{i}})\right]$$
$$+ C_m\left[\frac{(v-1)}{k\beta}\sqrt{-\mathrm{i}}\mathrm{J}'_m(k\beta\sqrt{-\mathrm{i}}) + \mathrm{i}\mathrm{J}_m(k\beta\sqrt{-\mathrm{i}}) - \frac{(v-1)m^2}{k^2\beta^2}\mathrm{J}_m(k\beta\sqrt{-\mathrm{i}})\right]$$
$$+ D_m\left[\frac{(v-1)}{k\beta}\sqrt{-\mathrm{i}}\mathrm{Y}'_m(k\beta\sqrt{-\mathrm{i}}) + \mathrm{i}\mathrm{Y}_m(k\beta\sqrt{-\mathrm{i}}) - \frac{(v-1)m^2}{k^2\beta^2}\mathrm{Y}_m(k\beta\sqrt{-\mathrm{i}})\right]$$
$$- \frac{\omega^*}{\mu^*}\sum_{n=1}^{\infty}\phi_{mn}^*\frac{\varepsilon_{mn}^2\cosh(\varepsilon_{mn}(h/a))}{\beta^2(\beta^4 + \varepsilon_{mn}^4)}\left[\frac{(v-1)}{k\varepsilon_{mn}}\mathrm{J}'_m(k\varepsilon_{mn})\right.$$
$$\left. - \mathrm{J}_m(k\varepsilon_{mn}) - \frac{(v-1)m^2}{k^2\varepsilon_{mn}^2}\mathrm{J}_m(k\varepsilon_{mn})\right] = 0 \tag{19}$$

and

$$A_m\left[\left\{-\mathrm{i}+\frac{(v-1)m^2}{k^2\beta^2}\right\}\sqrt{\mathrm{i}}\,\mathrm{J}'_m(k\beta\sqrt{\mathrm{i}})+\frac{(1-v)m^2}{k^3\beta^3}\,\mathrm{J}_m(k\beta\sqrt{\mathrm{i}})\right]$$

$$B_m\left[\left\{-\mathrm{i}+\frac{(v-1)m^2}{k^2\beta^2}\right\}\sqrt{\mathrm{i}}\,\mathrm{Y}'_m(k\beta\sqrt{\mathrm{i}})+\frac{(1-v)m^2}{k^3\beta^3}\,\mathrm{Y}_m(k\beta\sqrt{\mathrm{i}})\right]$$

$$C_m\left[\left\{\mathrm{i}+\frac{(v-1)m^2}{k^2\beta^2}\right\}\sqrt{-\mathrm{i}}\,\mathrm{J}'_m(k\beta\sqrt{-\mathrm{i}})+\frac{(1-v)\ m^2}{k^3\beta^3}\,\mathrm{J}_m(k\beta\sqrt{-\mathrm{i}})\right]$$

$$D_m\left[\left\{\mathrm{i}+\frac{(v-1)m^2}{k^2\beta^2}\right\}\sqrt{-\mathrm{i}}\,Y'_m(k\beta\sqrt{-\mathrm{i}})+\frac{(1-v)m^2}{k^3\beta^3}\,Y_m(k\beta\sqrt{-\mathrm{i}})\right]$$

$$-\frac{\omega^*}{\mu^*}\sum_{n=1}^{\infty}\phi^*_{mn}\frac{\varepsilon^3_{mn}\cosh(\varepsilon_{mn}(h/a))}{\beta^3(\beta^4+\varepsilon^4_{mn})}\left[\left(-1-\frac{(1-v)m^2}{k^2\varepsilon^2_{mn}}\right)\mathrm{J}'_m(k\varepsilon_{mn})\right.$$

$$\left.+\frac{(1-v)m^2}{k^3\varepsilon^3_{mn}}\,\mathrm{J}_m(k\varepsilon_{mn})\right]=0, \tag{20}$$

where the notation $\omega^{*2}\equiv\mu\omega^2a^4/D$, $\mu^*\equiv\mu/\rho a$ and $\phi^*_{mn}\equiv \mathrm{i}a\sqrt{\mu/D}\phi_{mn}$ has been employed.

These are four inhomogeneous algebraic equations for the determination of the integration constants A_m, B_m, C_m and D_m as functions of ϕ_{mn}, which yield the deflection $\bar{\zeta}_m$ as a function of r and ϕ_{mn}. For the determination of the remaining constants ϕ_{mn} (m fixed, describing the considered angular mode), one can employ the free surface condition (4) and the compatibility condition (5), which result in

$$\sum_{n=1}^{\infty}\phi^*_{mn}\mathrm{J}_m\left(\varepsilon_{mn}\frac{r}{a}\right)\left\{\varepsilon_{mn}(g^*+\sigma^*\mu^*\varepsilon^2_{mn})\sinh\left(\varepsilon_{mn}\frac{h}{a}\right)\right.$$

$$\left.-\omega^{*2}\cosh\left(\varepsilon_{mn}\frac{h}{a}\right)\right\}=0\quad\text{in the range}\quad 0\leqslant\frac{r}{a}<k, \tag{21}$$

and

$$\sum_{n=1}^{\infty}\phi^*_{mn}\varepsilon_{mn}\sinh\left(\varepsilon_{mn}\frac{h}{a}\right)\mathrm{J}_m\left(\varepsilon_{mn}\frac{r}{a}\right)+\omega^*\left\{A_m\mathrm{J}_m\left(\beta\frac{r}{a}\sqrt{\mathrm{i}}\right)\right.$$

$$+B_m\mathrm{Y}_m\left(\beta\frac{r}{a}\sqrt{\mathrm{i}}\right)+C_m\mathrm{J}_m\left(\beta\frac{r}{a}\sqrt{-\mathrm{i}}\right)$$

$$+D_m\mathrm{Y}_m\left(\beta\frac{r}{a}\sqrt{-\mathrm{i}}\right)-\frac{\omega^*}{\mu^*}\sum_{n=1}^{\infty}\phi^*_{mn}\frac{\cosh(\varepsilon_{mn}(h/a))}{(\beta^4+\varepsilon^4_{mn})}$$

$$\left.\times\mathrm{J}_m\left(\varepsilon_{mn}\frac{r}{a}\right)\right\}=0\quad\text{in the range}\quad k\leqslant\frac{r}{a}\leqslant 1. \tag{22}$$

In these equations, $g^* \equiv g\mu a^3/D$, $\sigma^* \equiv \sigma a^2/D$ have been used; also $\beta^4 \equiv g^*/\mu^* - \omega^{*2}$. Upon introducing in these equations the values A_m, B_m, C_m and D_m as obtained by Kramer's rule from equations (17)–(20), equations (21) and (22) are only equations of the unknown constants ϕ^*_{mn}.

If one satisfies the free surface condition in the range $0 \leqslant r/a < k$ at certain freely chosen N_1 points and the compatibility condition at freely chosen $(N_2 + 1)$ points in the range $k \leqslant r/a \leqslant 1$, one obtains $(N_1 + N_2 + 1)$ homogeneous algebraic equations in $\phi_{mj}(j = 1, 2, \ldots, (N_1 + N_2 + 1))$ unknown constants, of which the vanishing coefficient determinant represents the coupled frequency equation for the determination of the approximate lower coupled frequencies of the hydroelastic system. One has to introduce in equation (21) for

$$r/a = n_1 k/N_1 \quad \text{with } n_1 = 0, 1, 2, \ldots, (N_1 - 1)$$

and in equation (22)

$$r/a = k + n_2(1 - k)/N_2 \quad \text{with } n_2 = 0, 1, 2, \ldots, N_2,$$

while the infinite series are replaced by a finite sum running from $n = 1$ to $(N_1 + N_2 + 1)$. Equations (21) render N_1 equations and equation (22) results in $(N_2 + 1)$ algebraic equations.

3.2. FORCED TRANSLATIONAL EXCITATION

If the hydroelastic structure-liquid system is excited translationally by $X_0 e^{i\Omega t}$, where X_0 is the excitation amplitude and Ω the forcing frequency, the side-wall boundary condition yields the expression

$$\partial\phi/\partial r = i\Omega X_0 e^{i\Omega t} \cos\varphi \quad \text{at } r = a. \tag{23}$$

With the extraction of this rigid-body motion by

$$\phi(r, \varphi, z, t) = e^{i\Omega t} \cos\varphi [\psi(r, z) + i\Omega X_0 r], \tag{24}$$

one has to solve the Laplace equation ($m = 1$)

$$\frac{\partial^2\psi}{\partial r^2} + \frac{1}{r}\frac{\partial\psi}{\partial r} - \frac{\psi}{r^2} + \frac{\partial^2\psi}{\partial z^2} = 0 \tag{25}$$

with boundary conditions

$$\partial\psi/\partial r = 0 \quad \text{at } r = a \quad \text{and} \quad \partial\psi/\partial z = 0 \quad \text{at } z = -h \tag{26}$$

and the conditions

$$g\frac{\partial\psi}{\partial z}-\Omega^2\psi+\frac{\sigma}{\rho}\frac{\partial^3\psi}{\partial z^3}=\mathrm{i}\Omega^3X_0r \quad \text{at } z=0 \quad \text{in the range } 0\leqslant r/a<k, \tag{27}$$

$$\Omega\bar{\zeta}_1=\frac{\partial\psi}{\partial z} \quad \text{at } z=0 \text{ in the range } k\leqslant\frac{r}{a}\leqslant 1, \tag{28}$$

where the plate deflection could be expressed ($m=1$) as

$$\bar{\zeta}_1(r,\varphi,t)=\bar{\zeta}_1(r)\mathrm{e}^{\mathrm{i}\Omega t}\cos\varphi\,. \tag{29}$$

The solution of equation (25) yields the expression

$$\psi(r,z)=\sum_{n=1}^{\infty}\psi_{1n}\cosh\left\{\frac{\varepsilon_{1n}}{a}(z+h)\right\}\mathrm{J}_1\left(\varepsilon_{1n}\frac{r}{a}\right) \tag{30}$$

with which the equation for the motion of the annular plate may be expressed as

$$\left[\frac{\mathrm{d}^2}{\mathrm{d}r^2}+\frac{1}{r}\frac{\mathrm{d}}{\mathrm{d}r}-\frac{1}{r^2}\right]^2\bar{\zeta}_1-\left(\frac{\Omega^2\mu-\rho g}{D}\right)\bar{\zeta}_1=-\frac{\mathrm{i}\Omega\rho}{D}\sum_{n=1}^{\infty}\psi_{1n}\cosh\left(\varepsilon_{1n}\frac{h}{a}\right)\mathrm{J}_1\left(\varepsilon_{1n}\frac{r}{a}\right) \tag{31}$$

and exhibits with $\bar{\beta}^4=a^4(\rho g-\mu\Omega^2)/D$ the solution

$$\bar{\zeta}_1(r)=A_1\mathrm{J}_1\left(\bar{\beta}\frac{r}{a}\sqrt{\mathrm{i}}\right)+B_1\mathrm{Y}_1\left(\bar{\beta}\frac{r}{a}\sqrt{\mathrm{i}}\right)+C_1\mathrm{J}_1\left(\bar{\beta}\frac{r}{a}\sqrt{-\mathrm{i}}\right)+D_1\mathrm{Y}_1\left(\bar{\beta}\frac{r}{a}\sqrt{-\mathrm{i}}\right)$$

$$-\frac{\mathrm{i}\rho\Omega a^4}{D}\sum_{n=1}^{\infty}\psi_{1n}\frac{\cosh(\varepsilon_{1n}(h/a))\mathrm{J}_1(\varepsilon_{1n}(r/a))}{\bar{\beta}^4+\varepsilon_{1n}^4}. \tag{32}$$

Introducing for $m=1$, $\bar{\beta}$ instead of β and Ω^* for ω^* one obtains from equations (17)–(20) four inhomogeneous algebraic equations for the determination of A_1, B_1, C_1 and D_1 as functions of ψ^*_{1n}. The compatibility condition (28) and the free surface condition (27) are then

$$\sum_{n=1}^{\infty}\psi^*_{1n}\mathrm{J}_1\left(\varepsilon_{1n}\frac{r}{a}\right)\left\{\varepsilon_{1n}(g^*+\sigma^*\mu^*\varepsilon_{1n}^2)\sinh\left(\varepsilon_{1n}\frac{h}{a}\right)\right.$$

$$\left.-\Omega^{*2}\cosh\left(\varepsilon_{1n}\frac{h}{a}\right)\right\}=-\Omega^{*3}X_0r \quad \text{in the range} \quad 0\leqslant\frac{r}{a}<k, \tag{33}$$

and

$$\sum_{n=1}^{\infty} \psi_{1n}^* \varepsilon_{1n} \sinh\left(\varepsilon_{1n}\frac{h}{a}\right) \mathrm{J}_1\left(\varepsilon_{1n}\frac{r}{a}\right) + \Omega^* \Bigg\{ A_1 \mathrm{J}_1\left(\bar{\beta}\frac{r}{a}\sqrt{\mathrm{i}}\right) + B_1 \mathrm{Y}_1\left(\bar{\beta}\frac{r}{a}\sqrt{\mathrm{i}}\right)$$

$$+ C_1 \mathrm{J}_1\left(\bar{\beta}\frac{r}{a}\sqrt{-\mathrm{i}}\right) + D_1 \mathrm{Y}_1\left(\bar{\beta}\frac{r}{a}\sqrt{-\mathrm{i}}\right)$$

$$- \frac{\Omega^*}{\mu^*} \sum_{n=1}^{\infty} \psi_{1n}^* \frac{\cosh(\varepsilon_{1n}(h/a))}{(\bar{\beta}^4 + \varepsilon_{1n}^4)} \mathrm{J}_1\left(\varepsilon_{1n}\frac{r}{a}\right) \Bigg\} = 0 \quad \text{in the range} \quad k \leqslant \frac{r}{a} \leqslant 1. \quad (34)$$

If one satisfies these conditions at given points r/a one has an inhomogeneous algebraic system for the determination of the response values $\psi_{1j}^*(j = 1, 2, \ldots, (N_1 + N_2 + 1))$ which, introduced into the above results, renders the response potential ϕ. With the free surface displacement $\zeta(r, \varphi, t)$ the kinematic condition

$$\partial\zeta/\partial t = \partial\phi/\partial z \quad \text{at } z = 0$$

yields the response of the free liquid surface as

$$\zeta(r, \varphi, t) = \frac{\mathrm{e}^{\mathrm{i}\Omega t}}{\mathrm{i}\Omega} \cos\varphi \frac{\partial\psi}{\partial z}\Big|_{z=0} = -\sum_{n=1}^{\infty} \frac{\psi_{1n}^*}{\Omega^*} \cosh\left(\varepsilon_{1n}\frac{h}{a}\right) \mathrm{J}_1\left(\varepsilon_{1n}\frac{r}{a}\right) \cos\varphi \mathrm{e}^{\mathrm{i}\Omega^*\tau}, \quad (35)$$

where $\tau \equiv t/(a^2\sqrt{\mu/D})$ is the dimensionless time. Introducing $\psi_{1n}^*(\Omega^*)$ results in the magnification function of the free surface.

4. OTHER BOUNDARY CONDITIONS OF THE ANNULAR PLATE

If the annular plate is still free on its inner rim, but *simply supported* at the cylindrical wall $r = a$, then equations (8) have to be replaced by

$$\bar{\zeta} = 0 \quad \text{and} \quad \frac{\partial^2\bar{\zeta}}{\partial r^2} + \nu\left(\frac{1}{r}\frac{\partial\bar{\zeta}}{\partial r} + \frac{1}{r^2}\frac{\partial^2\bar{\zeta}}{\partial\varphi^2}\right) = 0 \quad \text{at} \quad \frac{r}{a} = 1.$$

For a *guided* boundary at $r = a$ one has to replace equations (8) by

$$\frac{\partial\bar{\zeta}}{\partial r} = 0 \quad \text{and} \quad \frac{\partial}{\partial r}\left[\frac{\partial^2\bar{\zeta}}{\partial r^2} + \frac{1}{r}\frac{\partial\bar{\zeta}}{\partial r} + \frac{1}{r^2}\frac{\partial^2\bar{\zeta}}{\partial\varphi^2}\right] + \frac{(1-\nu)}{r}\frac{\partial}{\partial r}\left(\frac{1}{r}\frac{\partial^2\bar{\zeta}}{\partial\varphi^2}\right) = 0 \quad \text{at} \quad \frac{r}{a} = 1.$$

If the annular plate is *elastically supported* at $r = a$ then equations (8) have to be replaced by

$$\frac{\partial}{\partial r}\left[\frac{\partial^2\bar{\zeta}}{\partial r^2} + \frac{1}{r}\frac{\partial\bar{\zeta}}{\partial r} + \frac{1}{r^2}\frac{\partial^2\bar{\zeta}}{\partial\varphi^2}\right] + \frac{(1-\nu)}{r}\frac{\partial}{\partial r}\left(\frac{1}{r}\frac{\partial^2\bar{\zeta}}{\partial\varphi^2}\right) = 0$$

and

$$\frac{\partial^2 \bar{\zeta}}{\partial r^2} + v\left(\frac{1}{r}\frac{\partial \bar{\zeta}}{\partial r} + \frac{1}{r^2}\frac{\partial^2 \bar{\zeta}}{\partial \varphi^2}\right) + \frac{K}{D}\frac{\partial \bar{\zeta}}{\partial r} = 0 \quad \text{at} \quad \frac{r}{a} = 1,$$

where the edge rotation is opposed by torsional springs having a distributed stiffness K (moment per unit length). In the case of a freely floating annular plate exhibiting free–free boundary conditions equations (9a) and (9b) have to be satisfied at $r/a = k$ and 1. The procedure for the solution is very similar to that shown in the previous sections.

It is worth mentioning that other coverage configurations, such as a circular plate concentrically located on the free liquid, may also be treated by a procedure very similar to that presented above.

5. NUMERICAL EVALUATIONS AND DISCUSSION

Some of the above obtained analytical results have been evaluated numerically. In the following numerical evaluation $N_1 + N_2 + 1$ was mostly in the range of 20–30, depending on the magnitude of b/a. The maximum value employed for it was 60. The convergence is adequate and it resulted in accurate results (for the given points) up to the third digit.

In Figure 2, ($a = 1$ m) the change of the fundamental natural frequency by the presence on an annular rigid ring structure on the free liquid surface is shown. The indicated parameter is the Bond number $\text{Bo} \equiv \rho g a^2/\sigma$, which ranges from 1 to 10^3. The liquid height ratio is given by $h/a = 2{\cdot}0$, while the mass density ρ has been chosen to be $\rho = 10^3$ kg/m^3 and the liquid surface tension is that of water and

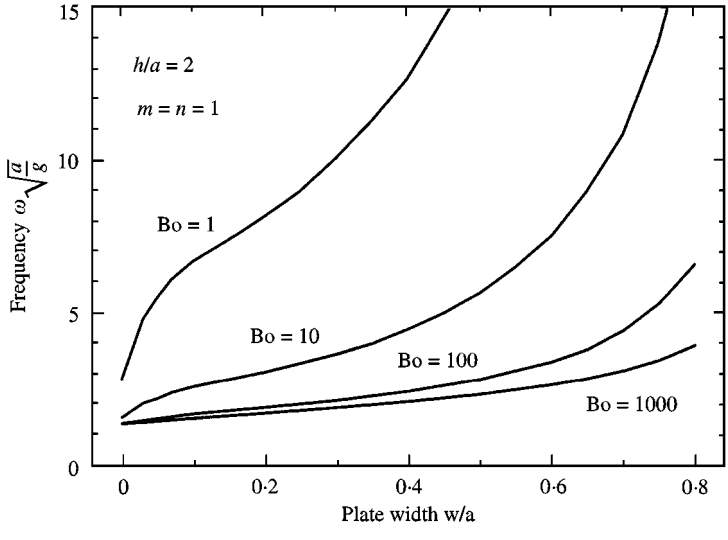

Figure 2. Lateral sloshing ($m = 1$, $n = 1$) frequencies for rigid annular plate coverage as a function of width of plate w/a ($h/a = 2{\cdot}0$, $\rho = 10^3$kg/m^3, $\sigma = 0{\cdot}0727$ N/m).

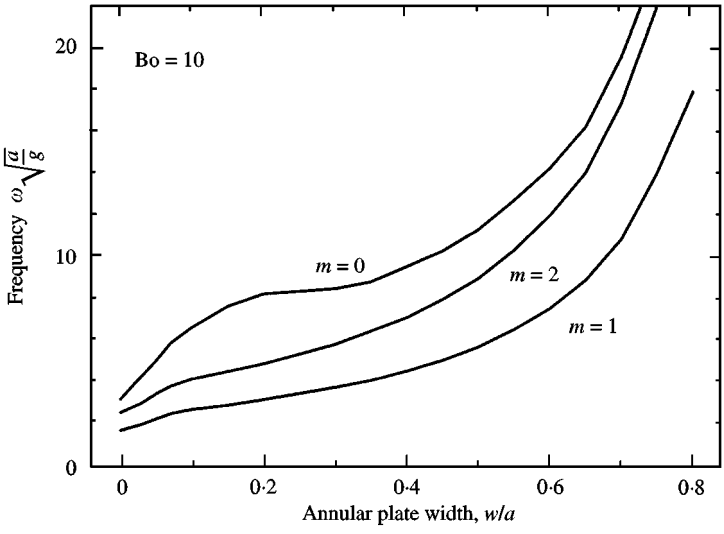

Figure 3. Sloshing frequency at Bo = 10 as a function of width of a rigid annular plate ($h/a = 2{\cdot}0$, $\rho = 10^3$ kg/m^3, $\sigma = 0{\cdot}0727$ N/m).

exhibits the magnitude $\sigma = 7{\cdot}27 \times 10^{-2}$ N/m. We note first of all that the natural frequency exhibits larger value for small Bond numbers and shows increased magnitude for increasing plate width w/a. If the free surface is not at all covered by a ring structure, i.e., $w/a = 0$, then the natural frequencies may be obtained from the well known natural frequency equation for a circular cylinder, i.e.,

$$\omega_{mn}^{*2} = \omega_{mn}^2 \frac{a}{g} = \varepsilon_{mn}\left(1 + \frac{\varepsilon_{mn}^2}{Bo}\right) \tanh\left(\varepsilon_{mn}\frac{h}{a}\right),$$

and may be seen at the location $w/a = 0$ in Figure 2. The large increase of the natural frequency with increasing plate width suggests also that the motion of the liquid in the container shall, as a result of the plate, be drastically reduced, a fact that has been noted previously [13].

In Figure 3, the natural frequencies for a rigid annular plate of width w for the Bond number Bo = 10 for the angular modes $m \leqslant 2$ are shown. The axisymmetric mode $m = 0$ exhibits the largest frequency and the largest change with increasing plate width w/a. The mode $m = 1$ with a nodal line at $\varphi = \pi/2, 3\pi/2$ is the most dangerous mode of sloshing since it exhibits the lowest natural frequency, usually too close to the control frequency of an aerospace vehicle. But here one can notice also a large increase of its magnitude as the plate width w/a increases, which calms down the motion of the liquid. The mode $m = 2$, exhibited according to $\cos 2\varphi$ radial nodal lines at $\varphi = \pi/4, 5\pi/4$ and $\varphi = 3\pi/4$ and $7\pi/4$, shows also larger natural frequencies as w/a increases. Similar results are presented in Figure 4 for the Bond number Bo = 100.

The effect of flexibility and the interaction of the elastic annular plate with the liquid has been evaluated numerically. If there is no liquid, the natural frequencies

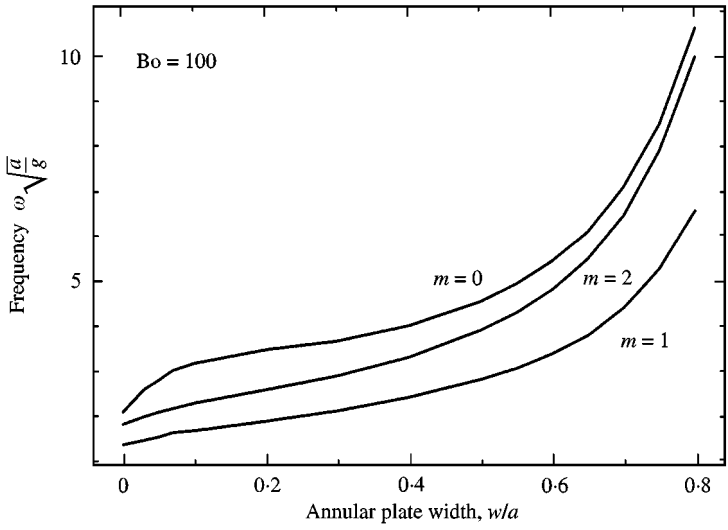

Figure 4. Sloshing frequency at Bo = 100 as a function of width of a rigid annular plate ($h/a = 2{\cdot}0$, $\rho = 10^3$ kg/m^3, $\sigma = 0{\cdot}0727$ N/m).

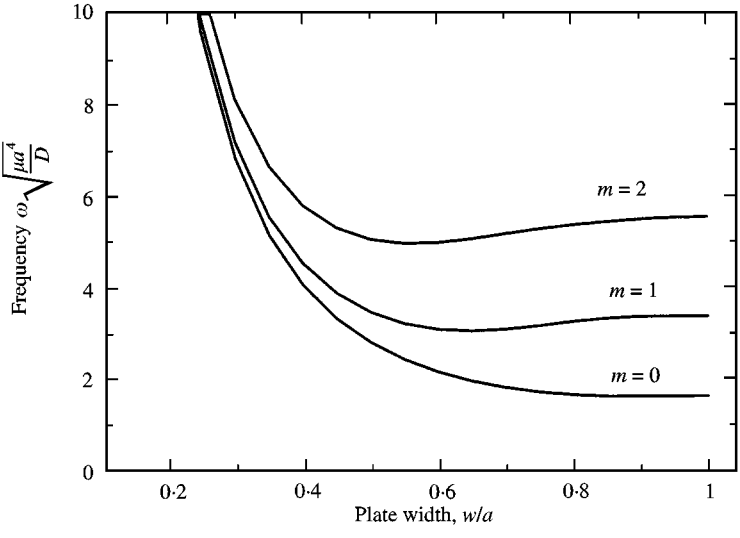

Figure 5. Natural (uncoupled) frequencies of elastic annular plate as a function of width w/a.

of the annular plate alone may be seen in Figure 5, where $\omega\sqrt{\mu a^4/D} = \lambda_{mn}^2$ is represented as a function of the width of the annular plate w/a. One can notice that with increasing width the natural frequencies decrease. These results may be found from equations (17)–(20) by omitting the influence of the liquid, i.e., omitting the infinite series on equations (19) and (20) and observing β^4 as $\lambda^4 = \mu\omega^2 a^4/D$ ($\rho \equiv 0$).

In Figure 6, are presented the coupled frequencies for $m = 1$ and the Bond number Bo = 10. The liquid height ratio has been chosen to be $h/a = 2.0$, the

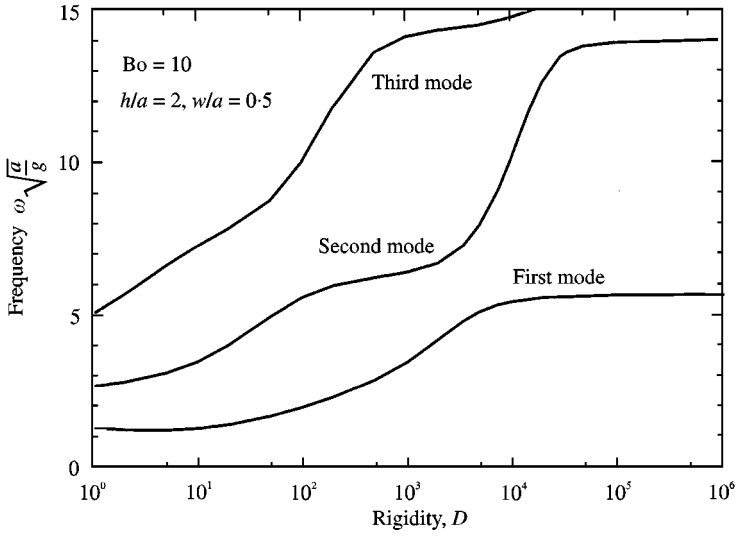

Figure 6. Coupled lateral ($m = 1$) mode frequencies at Bo = 10 as a function of rigidity D ($h/a = 2.0$, $w/a = 0{\cdot}5$, $\rho = 10^3$ kg/m^3, $\sigma = 0{\cdot}0727$ N/m, $\mu = 2700$ kg/m^3, $\nu = 1/3$, $E = 7 \times 10^{10}$ N/m^2)

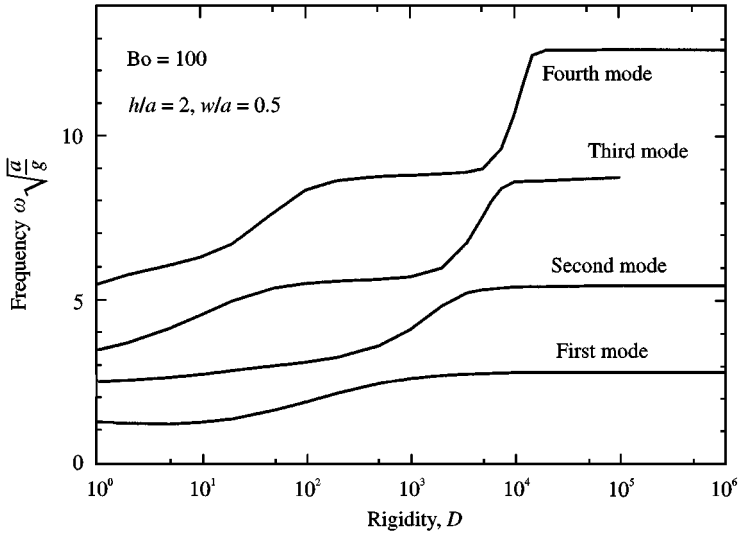

Figure 7. Coupled lateral ($m = 1$) mode frequencies at Bo = 100 as a function of rigidity D ($h/a = 2{\cdot}0$, $w/a = 0{\cdot}5$, $\rho = 10^3$ kg/m^3, $\sigma = 0.0727$ N/m, $\mu = 2700$ kg/m^3, $\nu = 1/3$, $E = 7 \times 10^{10}$ N/m^2).

Poisson ratio $\nu = \frac{1}{3}$, the liquid density $\rho = 10^3$ kg/m^3, the liquid surface tension $\sigma = 7{\cdot}27 \times 10^{-2}$ N/m, $\mu = 2700$ kg/m^3. With the increase of the rigidity D the coupled liquid frequency increases and reaches in the first mode for $D = 10^6$ (i.e., a nearly rigid annular plate of width $w/a = 0{\cdot}5$) the magnitude of about $\omega/\sqrt{g/a} \approx 5{\cdot}7$ as already obtained for a rigid plate in Figure 2. The more flexible the plate is, the more the decrease of the coupled sloshing frequency, an effect which defeats the purpose of the annular plate: i.e., the shifting of the natural frequency to

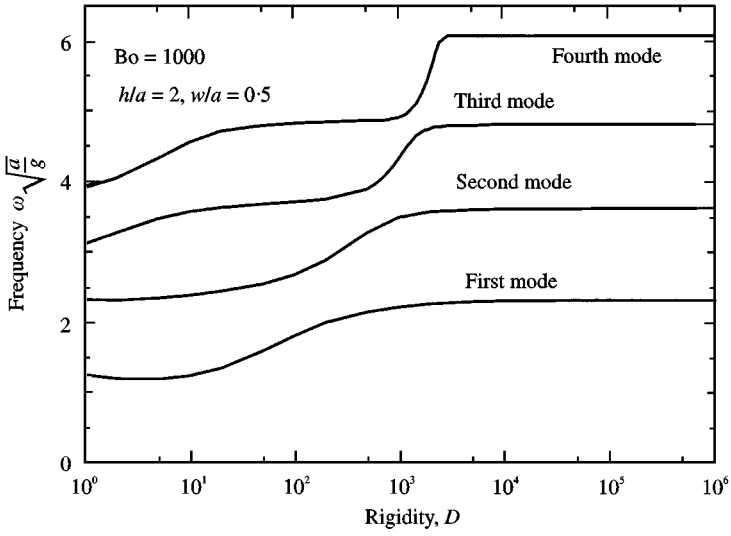

Figure 8. Coupled lateral ($m = 1$) mode frequencies at Bo = 1000 as a function of rigidity D ($h/a = 2{\cdot}0$, $w/a = 0{\cdot}5$, $\rho = 10^3$ kg/m^3, $\sigma = 0{\cdot}0727$ N/m, $\mu = 2700$ kg/m^3, $\nu = 1/3$, $E = 7 \times 10^{10}$ N/m^2).

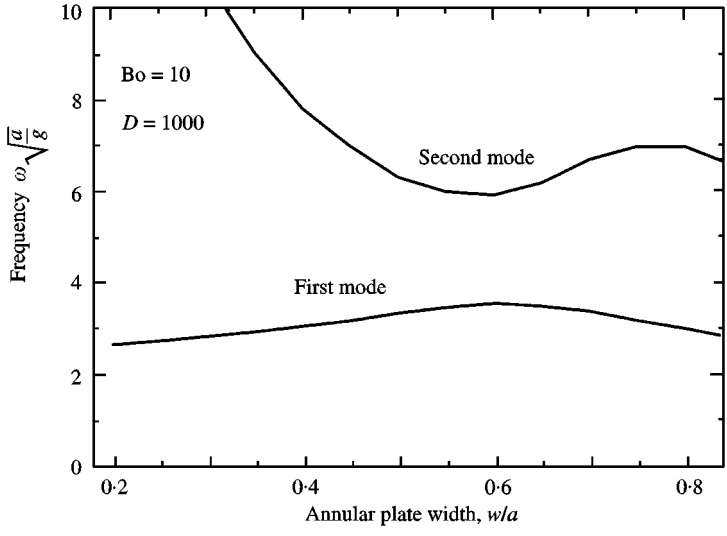

Figure 9. Coupled lateral ($m = 1$) mode frequencies at Bo = 10 and $D = 10^3$ as a function of width w/a of annular plate ($h/a = 2{\cdot}0$, $\rho = 10^3$ kg/m^3, $\sigma = 0{\cdot}0727$ N/m, $\mu = 2700$ kg/m^3, $\nu = 1/3$, $E = 7 \times 10^{10}$ N/m^2).

larger magnitudes and the calming down the motion of the liquid. One can notice, however, that a certain magnitude of $D(D > 10^2)$ is needed in order to have a valuable effect of the plate, since, if no plate is present, the natural frequency $\omega\sqrt{a/g} \approx 1{\cdot}6$ (see Figure 2 for Bo = 10) is larger than that for a plate of rigidity $D < 15$. In Figure 7, the result of the coupled sloshing frequency is presented for Bond number Bo = 100 and shows for $D = 10^6$ a value of about 2·85 (see Figure 2).

Again one may conclude that a very flexible baffle impairs the situation by exhibiting a coupled sloshing frequency smaller than the system without an annular baffle. In the latter case, $\omega\sqrt{a/g} \approx 1{\cdot}36$, while with a very elastic baffle it may be as low as 1·2. It may also be noticed that higher modes increase with increasing rigidity D and are exhibited from about $D = 10^4$ on nearly constant magnitude of the coupled frequencies. Figure 8 shows the same facts for a larger Bond number $\mathrm{Bo} = 1000$. The fundamental coupled mode exhibits for large rigidity D a coupled frequency of about 2·35 as may be found for a rigid annular plate from Figure 2 at $w/a = 0{\cdot}5$.

Finally, the coupled frequency for a Bond number $\mathrm{Bo} = 10$ and a rigidity $D = 1000$ is shown as a function of the width of the annular plate w/a in Figure 9. One can note that the lowest coupled mode shows a maximum of the coupled frequency at about $w/a \approx 0{\cdot}6$, exhibiting a coupled frequency of about $w\sqrt{a/g} \approx 3{\cdot}7$. Increased rigidity increases this frequency to about $w\sqrt{a/g} \approx 7{\cdot}7$ at $D \to \infty$.

6. CONCLUSIONS

1. A coverage of the free liquid surface by an annular plate increases the natural sloshing frequency and calms the motion of the liquid in the container. In addition, the participating sloshing masses are reduced, reducing the dynamic effect of propellant on the overall performance of the vehicle.
2. Increasing width of the obstructing annular plate increases the natural frequencies (valid for a rigid plate).
3. Increased Bond number $\mathrm{Bo} = \rho g a^2/\sigma$ exhibits also increased natural frequencies of the liquid.
4. With increasing rigidity D of the plate, the coupled natural frequencies increase. Plates that are too flexible do not show any benefit of increased coupled frequencies nor of calmed-down liquid motion.
5. Annular baffles will also exhibit a beneficial effect on the pressurization system of a cryogenic propellant system, inasmuch as it shows an inhibited cooling of the gaseous space of the container.

REFERENCES

1. H. F. Bauer 1964 *Zeitschrift für Flugwissenschaften* **12**, Part I, 85–101 und Part II, 222–229. Treibstoffschwingungen in Raketenbehältern und ihr Einfluss auf die Gesamtstabilität.
2. H. F. Bauer 1965 *Raumfahrtforschung* **9**, 76–90. Zum Zusammenwirken struktureller Schwingungen, Treibstoffschwappen und der Regelfrequenz bei Trägerraketen.
3. H. N. Abramson (editor) 1966 *NASA SP*-106. The dynamic behavior of liquids in moving containers.
4. H. F. Bauer and J. Villenueva 1967 *Lockheed-Georgia Company Report* No. ER-8798. Theory of liquid sloshing in a rectangular container with numerical examples for C5-wing.
5. E. W. Graham and A. M. Rodriguez 1952 *Journal of Applied Mechanics* **19**, 381–388. The characteristics of fuel motion which affect airplane dynamics.

6. H. F. Bauer 1981 *Zeitschrift für Flugwissenschaften und Weltraumforschung* **5**, 248–253. Freie Schwingungen in Parabolischen Behälterformen.
7. B. Budiansky 1960 *Journal of Aerospace Science* **27**, 161–173. Sloshing of liquids in circular canals and spherical tanks.
8. W.-H. Chu 1964 *American Institute of Aeronautics and Astronautics Journal* **2**, 1972–1979. Fuel sloshing in a spherical tank filled to an arbitrary depth.
9. H. F. Bauer 1982 *Acta Mechanica* **43**, 185–200. Flüssigkeitsschwingungen in Kegelbehältern.
10. H. F. Bauer and W. Eidel 1989 *Ingenieur-Archiv* **59**, 371–381. Liquid oscillations in a prolate spheroid.
11. H. F. Bauer 1963 *American Institute of Aeronautics and Astronautics Journal* **1**, 2601–2606. Liquid sloshing in a cylindrical quarter tank.
12. H. F. Bauer 1964 *American Institute of Aeronautics and Astronautics Journal* **2**, 768–770. Liquid sloshing in 45-degree compartmented sector tanks.
13. H. F. Bauer and W. Eidel 1999 *Aerospace Science and Technology*. Frictionless liquid sloshing in circular cylindrical container configurations, (accepted).
14. J. Siekmann and U. Schilling 1974 *Z. Flugwissenschaften* **22**, 168–173. Calculation of the free oscillations of a liquid in motionless axisymmetric containers of arbitrary shape.
15. D. O. Lomen 1965 *NASA-CR*-230 Digital analysis of liquid Propellant sloshing in mobile tanks with rotational symmetry.
16. H. J.-P. Morand and R. Ohayon 1995 *Fluid Structure Interaction*. New York: Wiley.

APPENDIX A: NOMENCLATURE

a	radius of container and outer radius of annular plate
b	inner radius of annular plate
$\mathrm{Bo} = \rho g a^2/\sigma$	Bond number
$D = E\delta^3/12(1-\nu^2)$	flexural rigidity of plate
E	Young's modulus of elasticity
g	gravity constant ($g^* \equiv g\mu a^3/D$)
h	liquid height
J_m, Y_m	Bessel Functions of mth order
$k = b/a$	diameter ratio
K	spring stiffness of torsional spring
p	liquid pressure
r, φ, z	polar co-ordinates
t	time
X_0	excitation amplitude
w	width of annular plate $w = a(1-k)$
$\beta^4 = a^4(\rho g - \mu\omega^2)$	
$\bar{\beta}^4 = a^4(\rho g - \mu\Omega^2)$	
δ	thickness of plate
ν	the Poisson ratio
ε_{mn}	zeros of $\mathrm{J}'_m(\varepsilon) = 0$
μ	mass per unit area of plate ($\mu^* \equiv \mu/\rho a$)
ρ	liquid mass density
ω	frequency ($\omega^{*2} \equiv \mu\omega^2 a^4/D$)
Ω	forcing frequency ($\Omega^{*2} \equiv \mu\Omega^2 a^4/D$)
σ	liquid surface tension ($\sigma^* \equiv \sigma a^2/D$)
ϕ	velocity potential